

# Drop breakage in a coalescence-dispersion pulsed-sieve-plate extraction column

G.S. Luo\*, H.B. Li, X.J. Tang, J.D. Wang

State Key Lab of Chemical Engineering, Department of Chemical Engineering, Tsinghua University,  
Beijing 100084, China

Received 10 December 2001; received in revised form 30 March 2004; accepted 2 April 2004

## Abstract

The droplet breakage in a coalescence-dispersion pulsed-sieve-plate extraction column (CDPSEC) was studied with 30%TBP (in kerosene)—water as a working system, and the organic phase as the dispersed phase. Because of the periodically arranged plates of every one coalescence plate with three dispersion plates in the CDPSEC, the droplets could coalesce and break up periodically. The drop size and its distribution were not kept at the constant values along the height of the column. It was found that the initial drop size distribution generated by the coalescence plate could be described with a normal distribution function. A mathematical model based on the population balance theory was developed to describe the drop size distribution along the column if only the drop breakage was considered when drops passed through the dispersion plates. The mean drop size and its distribution calculated by the model were in good agreement with the experimental results.

© 2004 Elsevier B.V. All rights reserved.

**Keywords:** Coalescence-dispersion pulsed-sieve-plate extraction column (CDPSEC); Breakage; Population balance model; Drop size distribution

## 1. Introduction

In a pulse-sieve-plate extraction column (PSEC), the breakage and coalescence of droplets greatly affect the drop size, the distribution and the holdup of the dispersed phase, which determine the throughput and the mass transfer performance. In order to describe the behavior of droplets as real as possible, the population balance model was developed in 1960s [1,2]. Garg and Pratt [3] and Mohanty Vogelpohl [4] applied the model to simulate and predict the hydrodynamics in a PSEC. Gourdon et al. [5] reviewed the applications of this model to various types of extraction columns.

It is of great importance to investigate the drop breakage and coalescence when the population balance model is applied to simulate the drop size distribution in PSEC. Gourdon et al. [5] suggested that there should be a maximum stable drop diameter below which the breakage probability of all the droplets was zero and developed a correlation in the form as  $d_{\max\text{stab}} \approx \varepsilon_m^{0.25}$  to calculate the maximum stable drop diameter. Molag et al. [6], Hancil and Rod [7] and Valentas and Amundson [8] assumed that it was possible

to break up for all the droplets and defined the drop breakage frequency as  $R(m) = km^{3/n}$  to investigate the breakage of droplets with different sizes. Casamatta and Vogelpohl [9] developed a correlation as  $R(d) = kd^\alpha$  to calculate the drop breakage frequency. Mlyenk and Resnick [10] indicated that the drop breakage probability could be defined as  $p(d) = \exp[-C/We(d)]$ . In most cases, the drop breakage was assumed to be binary breakage which meant that the mother drop could only break into two daughter droplets. The Beta function was usually applied to describe the daughter drop size distribution function [5,11–13]. In contrast to the drop breakage, the drop coalescence is more difficult to investigate for its complexities. Tobin and Ramkrishna [15] developed a model of drop coalescence considering the electrostatic repulsion effect. Ban et al. [14] investigated the influence of mass transfer directions and solute concentrations on the drop coalescence time. Simon and Bart [13] obtained the coalescence probability of droplets with different sizes in a Venturi tube.

Although these papers have been published to describe the droplet breakage and coalescence in the extraction columns, the comprehension in this area is still limited. Due to the poor understanding of the drop breakage and coalescence, the design and scale-up of extraction columns mainly and will continuously depend on extensive pilot-plant work, especially

\* Corresponding author. Tel.: +86 10 62770304; fax: +86 10 62770304.  
E-mail address: gsluo@tsinghua.edu.cn (G.S. Luo).

### Nomenclature

|                   |  |
|-------------------|--|
| $A$               | pulse amplitude (trough-to-peak) (cm)                  |
| $C$               | constant in Eq. (3)                                    |
| $d$               | drop diameter (m or mm)                                |
| $d_{32}$          | Sauter diameter (m or mm)                              |
| $d_{43}$          | mean diameter (m or mm)                                |
| $e$               | free area  |
| $f$               | pulse frequency ( $s^{-1}$ )                           |
| $F(i)$            | volumetric fraction                                    |
| $H$               | height (cm)  |
| $H_p$             | plate spacing (m)                                      |
| $n$               | drop number  |
| $p(i)$            | probability of breakage                                |
| $P(d)$            | volumetric probability density function ( $m^{-1}$ )   |
| $u_c$             | superficial velocity of continuous phase ( $ms^{-1}$ ) |
| $u_d$             | superficial velocity of dispersed phase ( $ms^{-1}$ )  |
| $We_p(i)$         | Weber particle number                                  |
| <i>Greek</i>      |  |
| $\beta(d, d_i)$   | daughter volumetric probability density function       |
| $\gamma$          | interfacial tension ( $N m^{-1}$ )                     |
| $\rho_c$          | density of continuous phase ( $kg m^{-3}$ )            |
| $\varepsilon$     | surface energy (J)                                     |
| $\varepsilon_m$   | dissipation rate per unit mass ( $m^2 s^{-3}$ )        |
| $\sigma$          | standard deviation ( $m^{-1}$ )                        |
| <i>Subscripts</i> |  |
| $i$               | drop class   |
| $j$               | drop class   |
| $k$               | elementary height no.                                  |

for the column with new structures. The focus of the research is to clarify the droplet breakage and coalescence and to develop the two-phase flow mathematical model [16].

A high performance extraction column called coalescence-dispersion PSEC (CDPSEC) has been developed in our laboratory. The CDPSEC is one of the improved columns over the standard PSEC. It was reported that the throughput of the CDPSEC was increased by 100%, and the overall mass transfer efficiency by 20% [17,18]. In CDPSEC, there are two different types of plates made of different materials, whose wetting abilities to the dispersed phase are different. The plate with better wetting ability to the dispersed phase is named as the coalescence plate, the other one named as the standard plate or dispersion plate. The coalescence plates are periodically inserted into the CDPSEC to replace parts of the standard plates. Therefore the droplets coalesce and break up periodically along the height of the column. Till now no research has been carried out to model this

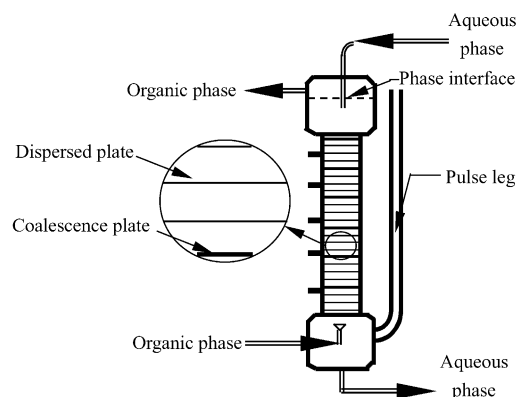


Fig. 1. The experimental set-up.

Table 1  
The specifications of the plates

|                                   | Material        | Free area (%) | Thickness (mm) | Hole diameter in plate (mm) |
|-----------------------------------|-----------------|---------------|----------------|-----------------------------|
| Dispersion plate (standard plate) | Stainless steel | 23            | 1              | 3                           |
| Coalescence plate                 | Teflon          | 23            | 2              |                             |

phenomenon. Thus the droplet breakage and coalescence in the CDPSEC need to be studied in detail.

## 2. Experimental set-up

The CDPSEC was composed of a glass section, with 150 mm in diameter and an effective height of 2 m, as shown in Fig. 1. The plate spacing was 50 mm. Lei et al. proved that the CDPSEC showed better performances with the combination of one coalescence plate every four plates [19]. The same arrange of the plates as Lei's was applied in this work. The specifications of the plates are listed in Table 1, and the coalescence plates are shown in Fig. 2.

As shown in Fig. 1, the pulse leg was connected to the main body of the column. At the top of the pulse leg there was a triple valve, which was connected to compressed air, free air and the pulse leg alternatively. Under a normal operating condition, the pulse leg and the main body were full of liquid. The compressed air was pumped into



Fig. 2. Structure of the coalescence plate.

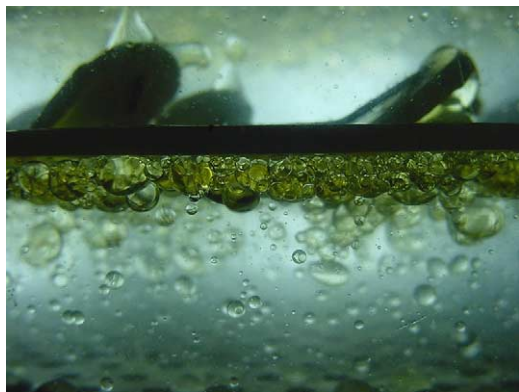


Fig. 3. Dispersed phase passing a coalescence plate.

the pulse leg at a certain frequency, and thus the pulsed flow in the CDPSEC was caused. By using a proportional-integral-derivative (PID) controller to control the two-phase interface position, the steady state operation could be easily reached.

The experimental system was 30%TBP (in kerosene)–nitric acid–water, and the organic phase as the dispersed phase. All the chemicals were purchased from Beijing Chemical Plant, and used directly without any further purification. The average drop size and its distribution were determined by taking photographs with a Kodak DC120 digital camera.

Figs. 3 and 4 are the photos of two-phase flow behavior under a certain operation condition in the CDPSEC.

Because of the different wetting abilities to the organic phase, the droplets coalesced, and broke up periodically along the height of the column. The average size and distribution of the droplets were not constant. After the dispersed phase passed through the coalescence plate, the mean drop size was likely to become larger. On the other hand, after the dispersed phase passed the dispersion plate, the droplet breakage played an important role, and the mean drop size was becoming smaller. Because the number of the dispersion plates was much more than that of the coalescence plates, the possibility of the droplet breakage was greater than that of the droplet coalescence.

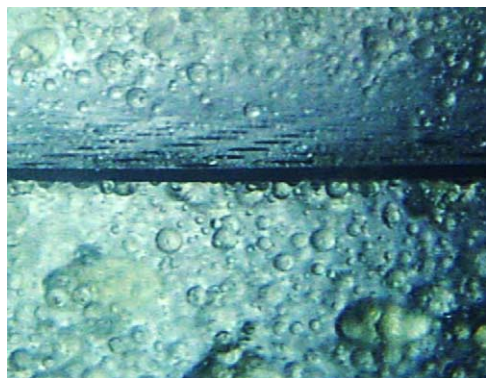


Fig. 4. Dispersed phase passing a coalescence plate dispersion plate.

### 3. Mathematical model

In this study, a simplified steady-state model is developed, based on the following assumptions:

- (1) The axial-mixing of the dispersed phase is neglected.
- (2) The drop coalescence happens only when the droplets pass through the coalescence plate.
- (3) An initial drop size distribution is defined as that after the droplets pass the coalescence plate. And the droplets break up only in the space between two coalescence plates.
- (4) Only the binary-breakage is assumed. It means that a drop can break up into two small droplets. The size of daughter droplets may be different.

The drop size range is divided into  $n$  uniform classes, which are  $d_1 < d_2 < d_3 < \dots < d_{n-1} < d_n$ .

According to the population balance model, the volumetric fraction balance for the droplet with diameter  $d_i$  in an elementary height  $\Delta h$  can be expressed as follows:

$$F_k(i) = F_{k-1}(i) - F_{k-1}(i)p(i) + \sum_{j>i}^n F_{k-1}(j)p(j)\beta(d_j, d_i) \quad (k = 1, 2, 3, \quad i = 1, 2, 3, \dots, n) \quad (1)$$

where  $F_k(i)$  is the volumetric fraction of  $d_i$  in elementary height  $k$ ,  $F_{k-1}(i)$  is the volumetric fraction of  $d_i$  from elementary height  $k-1$ ,  $p(i)$  is the breakage probability of  $d_i$ , and  $\beta(d_j, d_i)$  is the size distribution function of daughter droplets.

The volumetric fraction  $F(i)$  is defined as the volumetric fraction of the droplets with the diameter range in  $d(i) \pm \Delta d/2$ :

$$F(i) = P(d_i)\Delta d \quad (2)$$

where  $P(d_i)$  is the volumetric probability density function.

The breakage probability of  $d_i$  droplet is defined as Eq. (3) [10]:

$$p(i) = e^{-C/We_p(i)} \quad (3)$$

where  $C$  is a constant,  $We_p(i)$  is the Weber particle number ( $\rho_c \varepsilon_m^{2/3} d(i)^{5/3} / \gamma$ ,  $\varepsilon_m \approx C_3(Af)^3 / H_p$ ,  $C_3 = 5.82[(1 - e)(1 - e^2)/(e^2 C_4^2)]$ ,  $C_4 = 0.61$ ) [5]. According to Eq. (3), the larger the drop diameter is, the higher its breakage probability is.

As mentioned in the introduction, the daughter drop size distribution function is often assumed to be Beta function, but it is quite complex to apply. In this study, a new simplified method to predict daughter drop size distribution is developed instead of Beta function, based on the assumption that when the droplet breakage happens, the pulse energy is absorbed as much as possible, then converted to the surface energy to form the interface area to the best extent. It means that the more the formed interface area is, the more the volumetric probability density of daughter droplets is.

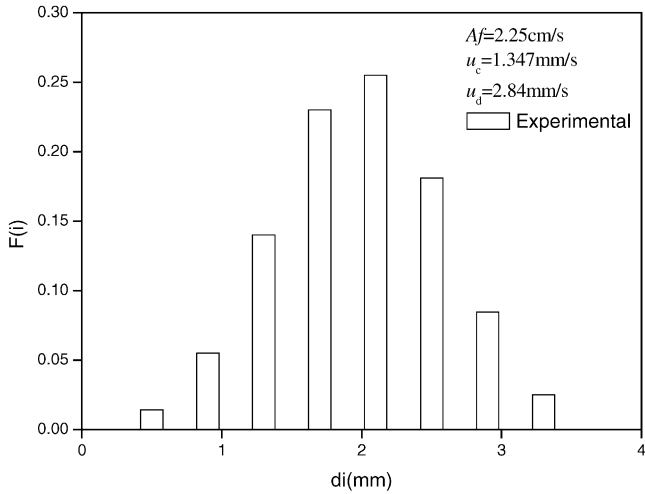


Fig. 5. Drop size distribution.

According to the assumption, when a droplet with diameter of  $d$  breaks into two droplets with diameter of  $d_i$  and  $d'_i$ , respectively, the surface energy increment  $\varepsilon_i$  is:

$$\varepsilon_i = \pi\gamma(d_i^2 + d'^2_i - d^2) \quad (4)$$

Thus the daughter volumetric probability density function  $\beta(d, d_i)$  is defined as Eq. (5):

$$\beta(d, d_i)\Delta d = \frac{\varepsilon_i}{\sum_{d_j < d} \varepsilon_j} \quad (5)$$

where  $\sum_{d_j < d} \varepsilon_j$  is the sum of the surface energy increments in all breakage cases of a drop with diameter in  $d$ . From Eq. (5), it can be seen that the volumetric probability density of daughter droplets is in direct proportion to the interface area generated from the drop breakage.

If the initial drop size distribution  $P(d_i)$ , generated from the coalescence plate, and the constant  $C$  in Eq. (3) are provided, the drop size distribution and the mean drop diam-

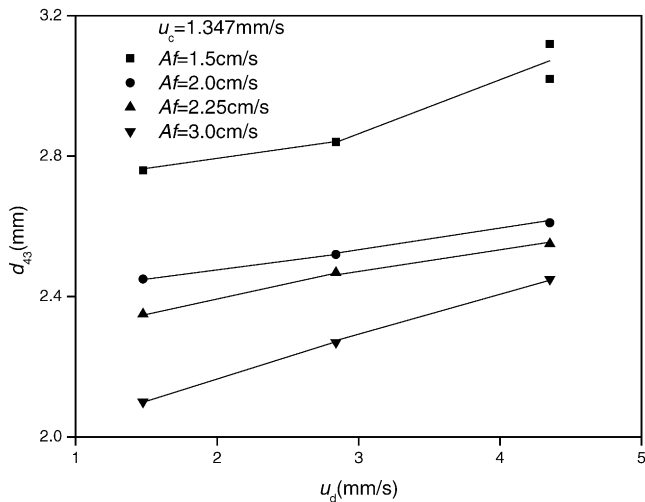


Fig. 6. Influence of operation conditions on  $d_{43}$ .

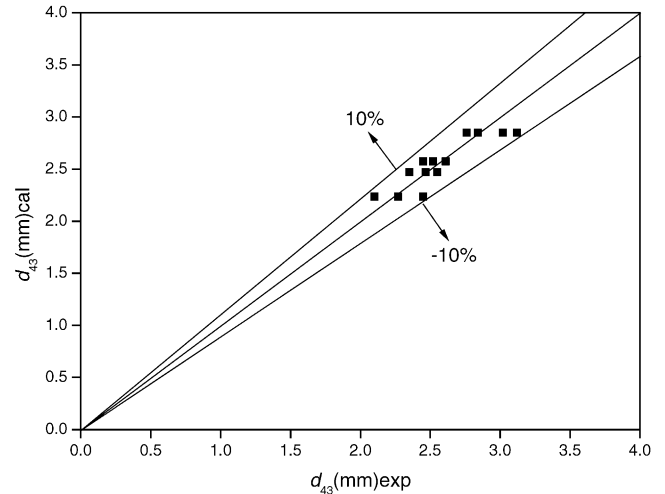


Fig. 7. Comparison between experimental data and calculated values.

eters along the height of the column can be calculated by using Eqs. (1)–(5).

The constant  $C$  in Eq. (3) can be evaluated from the experimental data with the following objective function:

$$\min J = \sum (d_{32_{\text{exp}}} - d_{32_{\text{cal}}})^2 \quad (6)$$

where  $d_{32_{\text{exp}}}$  is experimental and  $d_{32_{\text{cal}}}$  is calculated with Eq. (7):

$$d_{32_{\text{cal}}} = \frac{1}{\sum_{i=1}^n F_k(i)/d_i} \quad (7)$$

## 4. Results and discussion

### 4.1. Initial drop size distribution

As mentioned above, the initial drop size distribution is defined as that generated from the coalescence

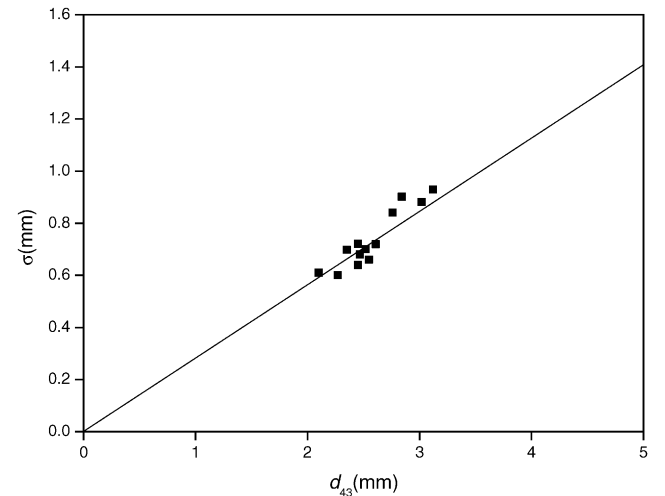


Fig. 8. Relationship between  $d_{43}$  and  $\sigma$ .

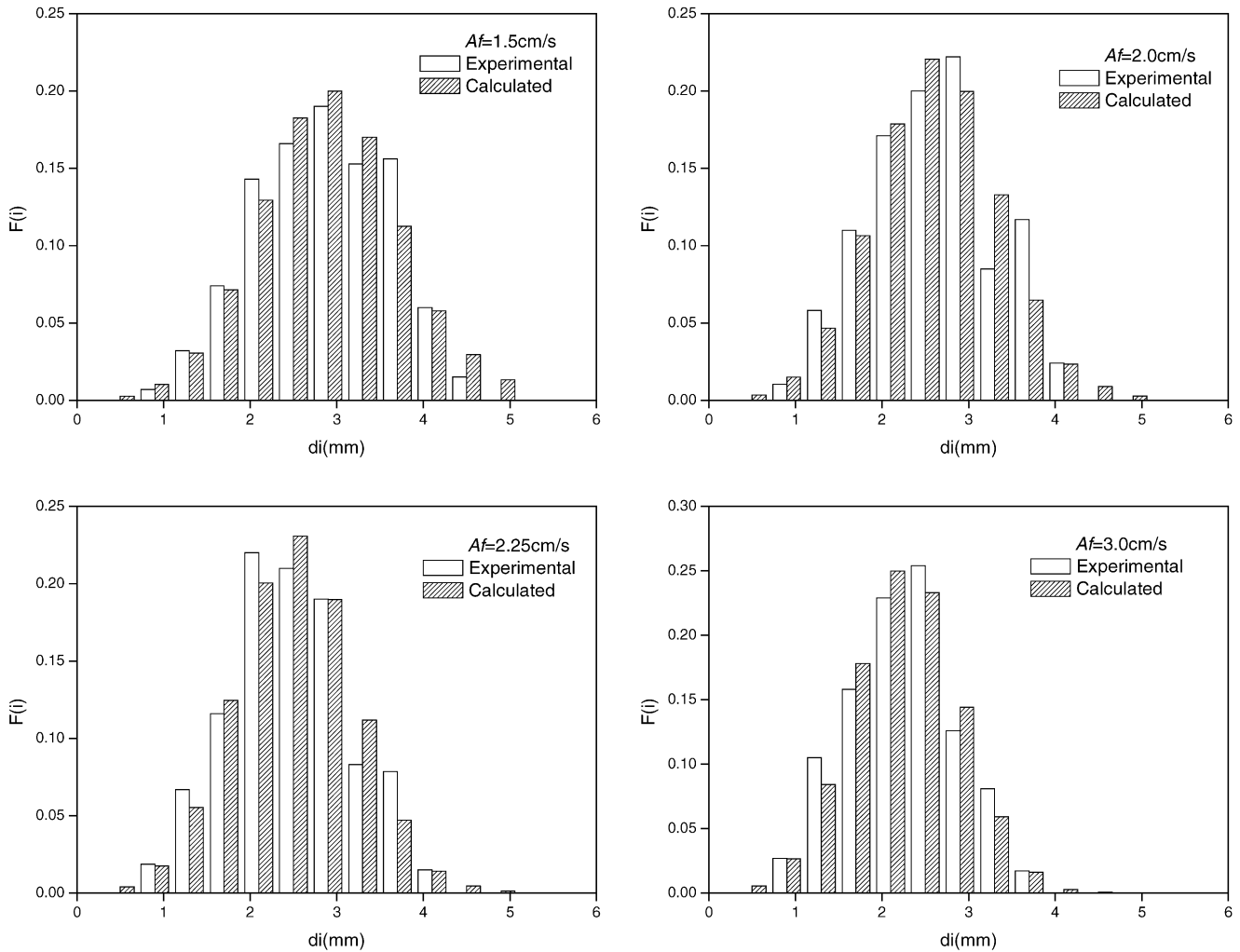


Fig. 9. Comparison between experimental data and calculated values.

plate. Fig. 5 shows a typical statistical result in the CDPSEC.

It can be found that the volumetric probability density function of the drops can be described with a normal distribution as Eq. (8):

$$P(d) = \frac{1}{\sqrt{2\pi}\sigma} \exp\left(-\frac{(d - d_{43})^2}{2\sigma^2}\right) \quad (8)$$

where

$$d_{43} = \int_0^\infty P(d)d \delta d = \sum_{i=1}^n \left( \frac{n_i d_i^4}{\sum_{j=1}^n n_j d_j^3} \right),$$

$$\sigma^2 = \int_0^\infty P(d)(d - d_{43})^2 \delta d = \sum_{i=1}^n \left( \frac{n_i d_i^3 (d_i - d_{43})^2}{\sum_{j=1}^n n_j d_j^3} \right)$$

The influence of the operating conditions on  $d_{43}$  is shown in Fig. 6. It was found that the influence of the pulse density ( $A_f$ ) was much greater than that of the flow rates. When  $A_f$  increased,  $d_{43}$  decreased. In order to predict the drop

size, a semi-empirical equation as Eq. (9) was given out by evaluating the experimental data:

$$d_{43} = 3.28 \times 10^{-3} (A_f)^{-0.35} \quad (9)$$

The comparison between  $d_{43,exp}$  and  $d_{43,cal}$  is shown in Fig. 7, and it can be seen that they fitted well with average deviation less than  $\pm 10\%$ .

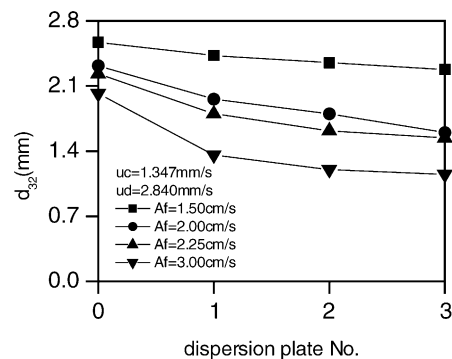


Fig. 10. Influence of  $A_f$  and positions on drop size.

Table 2  
Comparison of calculated data with the experimental results

| Dispersion plate no. | $Af = 1.5 \text{ cm/s}$ |                         | $Af = 2.0 \text{ cm/s}$ |                         | $Af = 2.25 \text{ cm/s}$ |                         | $Af = 3.0 \text{ cm/s}$ |                         |
|----------------------|-------------------------|-------------------------|-------------------------|-------------------------|--------------------------|-------------------------|-------------------------|-------------------------|
|                      | $d_{32\text{cal}}$ (mm) | $d_{32\text{exp}}$ (mm) | $d_{32\text{cal}}$ (mm) | $d_{32\text{exp}}$ (mm) | $d_{32\text{cal}}$ (mm)  | $d_{32\text{exp}}$ (mm) | $d_{32\text{cal}}$ (mm) | $d_{32\text{exp}}$ (mm) |
| 1                    | 2.45                    | 2.44                    | 1.98                    | 1.96                    | 1.80                     | 1.78                    | 1.38                    | 1.36                    |
| 2                    | 2.36                    | 2.35                    | 1.81                    | 1.80                    | 1.61                     | 1.62                    | 1.18                    | 1.20                    |
| 3                    | 2.29                    | 2.26                    | 1.69                    | 1.60                    | 1.50                     | 1.53                    | 1.08                    | 1.12                    |

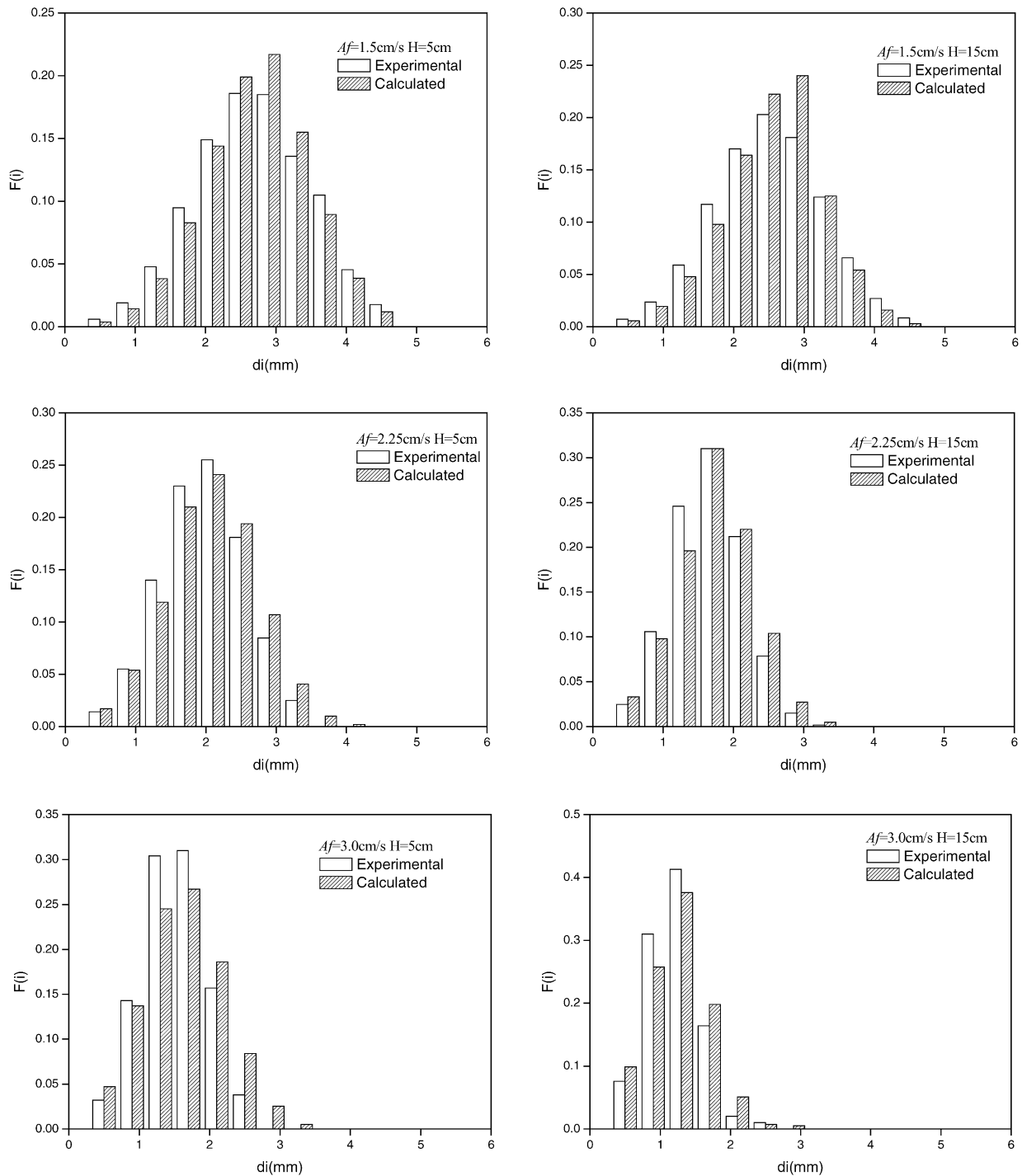


Fig. 11. Comparison of drop size distribution between experimental data and calculated values.



The relationship between  $d_{43}$  and  $\sigma$  is shown in Fig. 8. A linear relationship between  $d_{43}$  and  $\sigma$  can be seen. So Eq. (10) was given out to express the relationship:

$$\sigma = 0.28d_{43} = 9.18 \times 10^{-4}(Af)^{-0.35} \quad (10)$$

Therefore, if all operation conditions are provided, the initial drop size distribution in the CDPSEC can be obtained by using Eqs. (8)–(10). The comparison of the drop size distribution by calculation with these equations and that by experiments is shown in Fig. 9.

It can be seen that the normal distribution is a suitable function to predict the initial drop size distribution in the CDPSEC.

#### 4.2. Breakage of drops

Under different operating conditions, the mean drop size  $d_{32}$  will change greatly. Fig. 10 shows the influence of the operation conditions and positions on the drop size. As mentioned above, the drop size strongly depended on the pulse density  $Af$ . With an increase of  $Af$ , the drop size decreased. Moreover the drop size would decrease after the dispersed phase passed through the dispersion plate each time. In order to calculate the droplet breakage, the mathematical model in Section 3 was applied. With the experimental results, the constant  $C$  in Eq. (3) was evaluated, and the result of  $C = 0.395$  was obtained. The comparison of the experimental data and the calculated values by the model is shown in Table 2, and plotted in Fig. 11, which tell us that the mathematical model in Section 3 can predict the breakage of the droplets precisely.

### 5. Conclusions

The drop size distribution in the CDPSEC was studied in this work. Because of the existence of the coalescence plate, the droplets coalesced and broke up periodically in the CDPSEC. When the droplets passed through the coalescence plate, they coalesced into bigger droplets. When the droplets passed through the dispersion plate, they broke into smaller ones. The experimental results showed that the initial drop size distribution from the coalescence plate can be predicted with a normal distribution function, and the

mean drop size can be calculated with the equation of  $d_{43} = 3.28 \times 10^{-3}(Af)^{-0.35}$ . In order to describe the droplet breakage, a mathematical model based on the population balance theory has been suggested, and the parameters required in the model were evaluated. The comparison between the calculated values and the experimental data show that the mean diameter and the size distribution along the height of column can be calculated with the model satisfactorily.

### Acknowledgements

We acknowledge the support of the National Natural Science Foundation of China on this work.

### References

- [1] H.M. Hulburt, S.L. Katz, Chem. Eng. Sci. 19 (1964) 555.
- [2] K.J. Valentas, N.R. Amundson, Ind. Eng. Chem. Fund. 5 (1966) 533.
- [3] M.O. Garg, H.R.C. Pratt, AIChE J. 30 (1984) 432.
- [4] S. Mohanty, A. Vogelpohl, Chem. Eng. Prog. 36 (1997) 385.
- [5] C. Gourdon, G. Casamatta, G. Muratet, Population balance based modelling of solvent extraction column, in: J.C. Godfrey, M.J. Slater, (Eds), Liquid-Liquid Extraction Equipment, John Wiley & Sons, New York, 1994, p. 137.
- [6] M. Molag, G.E.H. Joosten, A.A.H. Drinkenburg, Ind. Eng. Chem. Fund. 19 (1980) 275.
- [7] V. Hancil, V. Rod, in: Proceedings of the Seventh CHISA Congress, Prague, 1981.
- [8] K.J. Valentas, N.R. Amundson, Ind. Eng. Chem. Fund. 5 (1966) 533.
- [9] G. Casamatta, A. Vogelpohl, Ger. Chem. Eng. 8 (1985) 96.
- [10] Y. Mlyenk, W. Resnick, AIChE J. 18 (1972) 122.
- [11] M.A. Hisa, L.L. Tavlarides, Chem. Eng. J. 26 (1983) 189.
- [12] S. Mohanty, A. Vogelpohl, Chem. Eng. Process. 36 (1997) 385.
- [13] M. Simon, H. Bart, Chem. Eng. Technol. 25 (2002) 481.
- [14] T. Ban, K. Fumio, S. Nii, K. Takahashi, Chem. Eng. Sci. 55 (2000) 5385.
- [15] T. Tobin, D. Ramkrishna, Can. J. Chem. Eng. 77 (1999) 1090.
- [16] S. Adler, E. Beaver, P. Bryan, J.E.L. Rogers, S. Robinson, C. Russomanno, Version 2020: 1998 Separations Roadmap, AIChE, New York, 1998.
- [17] X. Lei, Y.Y. Dai, Z.Y. Shen, J.D. Wang, in: Proceedings of the CIESC/AIChE Joint Meetings of Chemical Engineering, 1982, p. 538.
- [18] H.B. Li, G.S. Luo, W.Y. Fei, J.D. Wang, Chem. Eng. J. 78 (2000) 225.
- [19] X. Lei, Master thesis, Tsinghua University, China, 1981.